Incommensurate Phase Transitions and Anomalous Lattice Heat Capacities of Biphenyl†

Kazuya SAITO,†† Tooru ATAKE,††† and Hideaki CHIHARA*
Department of Chemistry and Chemical Thermodynamics Laboratory, Faculty of Science, Osaka University, Toyonaka, Osaka 560
(Received September 9, 1987)

Heat capacities of crystalline biphenyl were measured between 3 and 300 K by adiabatic calorimetry and some thermodynamic functions including the calorimetric standard entropy were tabulated. Thermodynamic properties of the successive phase transitions were determined; for the twist transition at (40.4±0.2) K, $\Delta_{trs}H$=(5.02±0.08) J·mol^{-1} and $\Delta_{trs}S$=(0.129±0.003) J·K^{-1}·mol^{-1}, and for the lock-in transition at (16.8±0.1) K, $\Delta_{trs}H$=(0.15±0.02) J·mol^{-1} and $\Delta_{trs}S$=(0.009±0.001) J·K^{-1}·mol^{-1}. Anomalously large heat capacities at low temperatures were analyzed based on lattice dynamics calculation, and the crossover of the low temperature heat capacities of biphenyl and *p*-terphenyl was attributed to the greater activity of the twisting mode in biphenyl. The relation of the bond flexibility to the incommensurability is discussed through the comparison of the low temperature heat capacities of biphenyl, *p*-terphenyl, and 4,4′-difluorobiphenyl.

Biphenyl is an interesting molecule which changes its conformation according as the state of aggregation changes. While molecules are twisted by about 40° about its central C–C bond in the gaseous state[1,2] and about 30° in the liquid state,[2–6] they crystallize in the structure of the space group $P2_1/a$ with the planar conformation at room temperature.[7–14] On cooling, however, they resume the twisted conformation below the phase transition temperature at about 40 K;[15–17] a similar phase transition, "twist transition," has also been found in *p*-terphenyl[18–21] and in *p*-quaterphenyl.[22,23]

The soft-modes have been found by optical[24–26] and neutron scattering[27] experiments. The softening occurs at the general point (x^*, y^*, z^*) near the B (0, 1/2, 0) point in the reciprocal space and the new phase is of two dimensionally incommensurate structure[28,29] classified to the five dimensional Bravais lattice of $P^{P2/m}_{cmm}$.[30] The modulation wave which characterizes this phase is expressed as $q^*=\pm(\delta_a a^*-\delta_c c^*)\pm 1/2\times(1-\delta_b)b^*$. The mean approximate structure was obtained neglecting satellite reflections in the diffraction diagram and was classified to Pa.[15] Dworkin and Cailleau[31] reported the results of their heat capacity measurements on biphenyl, in which they could not detect any anomaly in the heat capacity curve. On the other hand, Cullick and Gerkin[32] found the temperature halt at 42 K in the cooling curves, which strongly suggested that the transition is of the first-order. However, other authors[24–27,33–38] reported by making use of several experimental techniques that the transition is of higher-order.

On further cooling, the incommensurate-commensurate transition (so-called lock-in transition) in the one direction takes place at about 17 K,[28,29,34] i.e. δ_a and δ_c equal 0 below the lock-in transition. Below this transition, however, the crystal still remains incommensurate along the b^* axis. The structure was determined to be of the super-space group $P^{P2_1/a}_{1\bar{1}}$ by using neutron diffraction technique.[16] The essential aspect of the incommensurate modulation was a torsion about the central C–C bond with an amplitude of 5.5° for each phenyl ring, the maximum twisting angle being 11°. The lock-in transition has been revealed to be of the first-order by using optical[34] and neutron diffraction[28,38] techniques. More direct evidence of the first-order nature is the co-existence of the two phases observed in neutron experiments. On the other hand, no abrupt change was observed in Brillouin scattering experiments[36] and in electronic spectra of molecules.[35]

The lock-in transition in the direction of the b^* axis has not been observed so far down to 1.4 K.[38]

Dynamics in the incommensurate phases have been investigated by using some experimental techniques. The dispersion of the phason and the amplitudon branches were determined by neutron[27,40] and Brillouin[36] scattering experiments. The damping of the phason branch near the zone center was rather small. NMR results by Liu and Conradi[41] showed the existence of the slow process ($\tau\simeq 10^3$ s at 4.2 K) in the incommensurate phases. They proposed the term, "incommensurate glass," in biphenyl in the lowest temperature region. Recently, Benkert and Heine[42] interpreted the slow process as the shifting of the modulation boundaries.

It must be noted that the pressure dependence of the transition temperatures are negative.[37,43] This clearly shows that the transitions are connected with a subtle balance between intra- and intermolecular interactions.

Since Hochstrasser et al.[44] discovered the phase

† Contribution No. 130 from Chemical Thermodynamics Laboratory, Faculty of Science, Osaka University.

†† Present address: Department of Chemistry, Faculty of Science, Tokyo Metropolitan University, Fukazawa, Setagaya-ku, Tokyo 158.

††† Present address: Research Laboratory of Engineering Materials, Tokyo Institute of Technology, 4259 Nagatsuta-cho, Midori-ku, Yokohama 227.

transition in biphenyl crystal, many interesting features have been revealed by making use of several experimental techniques as briefly summarized above. Theoretical treatments[39,42,45-50] have also been presented based on these experimental results. However, accurate thermodynamic properties have been lacking although they should give an important clue to the nature of the transition and provide a critical test of theory. These situations led us to begin a series of thermodynamic studies on the successive phase transitions in crystalline biphenyl and related substances, parts of which were published elsewhere.[51-59] This paper provides the full description of precision heat capacity measurements. The anomalous lattice heat capacity at low temperatures will be analyzed by using the method of lattice dynamics.

Experimental

Commercially available biphenyl (Nakarai Chemicals, Ltd.) was purified by fractional sublimation in vacuum at room temperature. In order to avoid possible formation of metastable phases and/or poor crystallinity, the sublimed specimen was melted under a helium atmosphere (10^5 Pa) and cooled gradually down to room temperature for recrystallization. The purity of the specimen was better than 99.9 moles per cent as confirmed by gas chromatography.

The powdered specimen was loaded into the calorimeter vessel and sealed off with some helium gas for heat exchange (3 kPa at room temperature). The contribution of the helium gas to the total heat capacity was negligibly small. The mass of the sample used for calorimetry was 17.950 g (0.11640 mol). The contribution of the sample to the total heat capacity including that of the calorimeter vessel was larger than 70 per cent below 20 K. It decreased to 46 per cent at 100 K as temperature increased; however, it increased again to 59 per cent at 300 K.

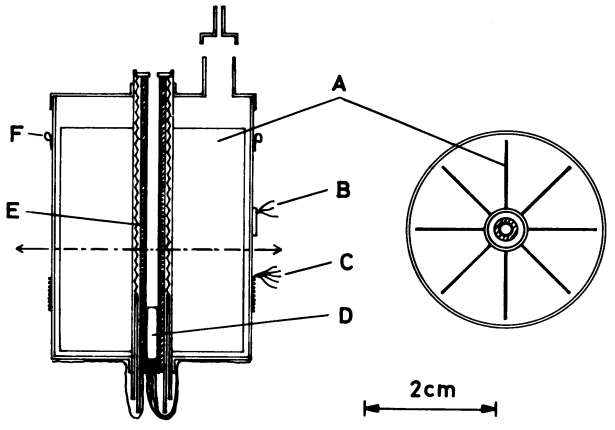

Fig. 1. Sectional plan of the new calorimeter vessel. A eight vanes to assist in thermal uniformity; B Au+0.07%Fe vs. Chromel-P thermocouples for adiabatic control (diameter 0.1 mm); C lead wires (diameter 0.1 mm); D germanium thermometer (model N2D, SI Inc.); E heater (KARMA, total 190 Ω); F hooks for hanging the vessel.

The apparatus for calorimetry has been described elsewhere.[59] A platinum resistance thermometer (model 8164, Leeds & Northrup Co.) and a germanium resistance thermometer (model CR-1000, CryoCal Inc.) were used. Their temperature scales are based on IPTS-68, helium gas thermometry, and the 1958 ^{4}He vapor pressure scale.[60,61]

The measurements using the ordinary calorimeter vessel failed to detect the lock-in transition at 16.8 K. To improve the sensitivity, a new calorimeter vessel was constructed with the following considerations; (1) use of a single, sensitive thermometer and one smooth temperature scale between 3 and 20 K, (2) amount of the sample that can be loaded and its packing in the vessel, and (3) attainment of better adiabatic conditions.

The sectional plan of the new calorimeter vessel (gold-plated copper) is shown in Fig. 1. In order to load a sufficient amount of the sample and to discard the use of helium gas for heat exchange in the vessel, the purified specimen was loaded and melted under a helium atmosphere (10^5 Pa) in the vessel before installation of the KARMA heater, the thermometer and thermocouples. The vessel was then evacuated and sealed off without addition of helium gas. The sample thus loaded weighed 24.957 g (0.16184 mol) in vacuum.

A germanium resistance thermometer (model N2D, SI Inc.) with commercial calibration was used. The calibration was based on the 1962 ^{3}He vapor pressure scale below 3.2 K and on the 1965 Provisional Helium Acoustic Scale between 2 and 20 K. The accuracy of the calibration was stated to be better than ±0.005 K below 5 K and better than ±0.01 K between 5 and 20 K. The 35 calibration points were fitted to the equation,

$$\ln(R/\Omega) = \sum_{i=1}^{9} A_i \{\ln(T/\mathrm{K})\}^{i-2}.$$

Since the main purpose of the measurements using this vessel was a search for the lock-in transition, an emphasis was placed on the smoothness of the temperature scale.

The Au+0.07%Fe vs. Chromel-P thermocouple (0.1 mm in diameter) was used for detecting the temperature difference between the vessel and the walls of adiabatic shield in order to improve the adiabatic conditions. The sensitivity of this thermocouple in the temperature region between 3 and 20 K is ten times as large as that of Chromel-P vs. Constantan thermocouple which has been attached to the ordinary vessel.

The new vessel thus constructed has an empty mass of 39.72 g with inside capacity of 25.06 cm^3. Other components of cryostat/calorimeter assembly were the same as used previously.[59] The sample contributed more than 85 per cent to the total heat capacity over the region studied (3—20 K) and the desired precision was attained.

Results and Discussion

Heat Capacities and Thermodynamic Functions.

The molar heat capacities measured with the ordinary (old) vessel are tabulated in Table 1 in the chronological order of measurement. The data obtained with the new vessel are shown as series 26 through 34 in Table 1. These were consistent with data obtained using the old vessel except for the lock-in

Table 1. Measured Molar Heat Capacities of Biphenyl

T	$C_{p,m}$	T	$C_{p,m}$	T	$C_{p,m}$	T	$C_{p,m}$	T	$C_{p,m}$
K	J K^{-1} mol^{-1}	K	J K^{-1} mol^{-1}	K	J K^{-1} mol^{-1}	K	J K^{-1} mol^{-1}	K	J K^{-1} mol^{-1}
Series 1		92.570	71.807	295.734	196.43	6.556	1.154	7.789	1.709
22.893	18.498	94.766	72.905	299.152	198.94	7.005	1.323	8.229	1.981
24.316	20.354	96.977	74.063	Series 15		7.477	1.570	8.712	2.302
25.736	22.177	99.242	75.199	14.181	7.506	8.013	1.899	9.238	2.678
27.178	24.002	101.587	76.333	14.921	8.365	8.621	2.295	9.805	3.118
28.647	25.811	103.975	77.585	15.769	9.351	Series 24		10.401	3.622
30.247	27.775	106.377	79.00	Series 16		5.591	0.723	11.021	4.149
31.954	29.863	108.758	80.24	18.738	12.984	5.940	0.851	11.642	4.665
33.668	31.832	Series 8		19.828	14.495	6.311	1.005	12.274	5.367
35.376	33.756	109.158	80.23	20.927	15.903	6.709	1.183	Series 31	
37.060	35.623	111.493	81.49	22.009	17.314	7.137	1.396	10.725	3.896
38.805	37.448	113.761	82.67	23.106	18.750	7.610	1.658	11.136	4.277
40.600	39.223	116.069	83.81	Series 17		8.154	1.992	11.581	4.696
42.342	40.689	118.417	85.02	14.089	7.394	8.781	2.414	12.056	5.154
44.038	41.926	120.787	86.27	14.847	8.290	9.479	2.935	12.571	5.672
45.727	43.163	123.163	87.46	15.635	9.197	10.256	3.582	13.164	6.292
47.417	44.462	125.545	88.57	16.467	10.202	11.114	4.319	13.807	6.999
49.116	45.762	Series 9		17.331	11.308	12.057	5.234	14.479	7.757
Series 2		125.967	88.83	18.232	12.452	13.030	6.186	15.210	8.628
22.785	18.352	128.403	90.10	19.183	13.661	13.963	7.228	15.964	9.569
24.241	20.261	130.793	91.31	20.109	14.847	Series 25		16.713	10.584
25.688	22.112	133.193	92.61	20.975	15.890	15.546	9.121	17.429	11.493
27.155	23.970	135.581	93.89	21.823	16.994	16.272	9.995	18.123	12.424
28.656	25.823	137.956	95.12	22.662	18.114	17.008	10.912	18.828	13.485
30.218	27.742	140.338	96.38	23.496	19.233	17.765	11.850	19.536	14.654
31.859	29.728	142.722	97.65	Series 18		18.551	12.850	20.250	18.386
33.493	31.639	145.104	98.95	4.051	0.300	19.372	13.893	Series 32	
35.048	33.404	Series 10		4.487	0.403	20.239	15.012	11.708	4.800
36.532	35.041	145.258	98.98	4.969	0.530	21.130	16.142	12.060	5.156
37.987	36.602	147.664	100.27	5.491	0.703	22.019	17.289	12.397	5.485
39.447	38.091	150.066	101.53	6.045	0.907	22.906	18.441	12.729	5.831
40.897	39.493	152.484	102.87	6.592	1.148	23.783	19.592	13.063	6.174
42.337	40.691	154.930	104.28	7.122	1.388	Seres 26		13.395	6.531
43.774	41.726	157.365	105.64	Series 19		6.543	1.057	13.722	6.895
45.209	42.796	159.778	106.99	3.855	0.243	6.928	1.234	14.049	7.258
46.657	43.873	162.177	108.36	4.224	0.332	7.403	1.487	14.377	7.633
48.132	45.001	Series 11		4.605	0.422	7.930	1.787	14.708	8.020
49.761	46.248	164.585	109.71	5.004	0.538	8.492	2.152	15.043	8.415
51.634	47.623	167.013	111.11	5.447	0.678	9.104	2.585	15.382	8.826
53.566	49.046	169.462	112.48	5.935	0.857	9.783	3.099	15.726	9.264
55.431	50.339	171.923	113.92	6.461	1.078	10.544	3.727	16.077	9.702
57.249	51.595	Series 12		7.003	1.334	11.394	4.499	16.431	10.180
59.027	52.793	172.821	114.52	Series 20		Series 27		16.784	10.688
60.796	53.955	175.305	116.04	4.443	0.382	4.105	0.288	17.139	11.117
Series 3		177.802	117.47	4.884	0.503	4.388	0.350	17.496	11.560
53.638	49.090	180.351	119.03	5.331	0.640	4.767	0.440	17.854	12.038
55.451	50.339	182.902	120.59	5.788	0.801	5.202	0.562	18.212	12.532
57.233	51.572	185.448	122.04	6.263	0.984	5.658	0.709	18.569	13.060
58.994	52.774	187.977	123.48	6.737	1.199	6.121	0.883	18.923	13.627
Series 4		190.505	125.01	7.243	1.453	6.591	1.083	19.273	14.174
32.858	30.907	193.048	126.59	7.805	1.775	7.063	1.309	19.629	14.794
34.022	32.239	195.582	128.11	8.434	2.174	7.541	1.567	19.978	15.454
35.130	33.482	198.157	129.76	9.146	2.676	8.043	1.871	Series 33	
36.186	34.659	Series 13		9.952	3.318	8.578	2.215	13.648	6.819
37.201	35.775	200.711	131.29	10.817	4.063	9.152	2.618	13.961	7.214
38.188	36.823	203.324	132.93	11.679	4.866	9.776	3.092	Series 34	
39.152	37.800	205.969	134.57	12.517	5.664	Series 28		14.244	7.472

Table 1. (Continued)

T	$C_{p,m}$	T	$C_{p,m}$	T	$C_{p,m}$	T	$C_{p,m}$	T	$C_{p,m}$
K	J K^{-1} mol^{-1}	K	J K^{-1} mol^{-1}	K	J K^{-1} mol^{-1}	K	J K^{-1} mol^{-1}	K	J K^{-1} mol^{-1}
40.094	38.742	208.606	136.40	13.353	6.568	10.453	3.656	14.459	7.727
41.031	39.619	211.190	137.97	Series 21		11.171	4.302	14.679	7.965
41.958	40.392	213.768	139.64	9.882	3.267	11.944	5.042	14.904	8.231
42.883	41.110	216.395	141.29	10.642	3.917	12.701	5.811	15.132	8.500
43.819	41.768	219.046	143.00	11.384	4.585	13.445	6.597	15.361	8.785
Series 5		221.726	144.89	12.110	5.269	14.171	7.401	15.591	9.066
60.493	53.726	224.437	146.63	12.836	6.012	14.890	8.244	15.822	9.351
62.242	54.872	227.180	148.49	13.576	6.779	15.606	9.101	16.053	9.661
63.980	55.960	229.946	150.29	Series 22		16.334	10.036	16.279	9.938
65.786	57.054	232.738	152.46	14.132	7.486	17.085	11.026	16.503	10.252
67.659	58.173	235.561	154.13	14.838	8.318	17.852	12.029	16.727	10.576
69.539	59.296	238.415	156.46	15.648	9.264	18.617	13.169	16.949	10.856
71.436	60.404	Series 14		16.532	10.340	19.357	14.279	17.169	11.137
73.337	61.494	241.166	157.68	17.451	11.490	20.057	15.732	17.390	11.391
75.222	62.533	244.021	159.79	18.406	12.691	Series 29		17.610	11.678
77.095	63.584	246.985	161.76	19.370	13.942	3.668	0.206	17.830	11.979
79.014	64.643	250.014	163.80	20.302	15.111	3.847	0.239	18.050	12.260
81.032	65.744	253.076	165.93	21.189	16.245	4.085	0.284	18.268	12.585
Series 6		256.170	168.01	22.041	17.365	4.389	0.348	18.487	12.899
81.058	65.822	259.302	170.31	22.865	18.432	4.740	0.434	18.706	13.233
83.133	66.814	262.477	172.48	23.667	19.481	5.126	0.540	18.924	13.559
85.160	67.875	265.702	174.70	Series 23		Series 30		19.142	13.955
87.174	68.926	268.951	177.13	3.594	0.222	3.686	0.207	19.359	14.299
89.175	70.030	272.209	179.02	3.907	0.288	3.878	0.244	19.576	14.684
91.166	71.037	275.491	181.90	4.164	0.327	4.128	0.293	19.793	15.058
Series 7		278.789	184.12	4.520	0.401	4.449	0.363	20.009	15.530
90.405	70.652	282.116	186.40	4.909	0.503	4.835	0.458		
		285.481	188.86	5.312	0.631	5.258	0.579		
		288.879	191.59	5.719	0.774	5.694	0.723		
		292.304	193.93	6.131	0.938	6.129	0.887		
						6.556	1.067		
						6.969	1.263		
						7.375	1.475		

The ordinary calorimeter vessel was used in series 1 through 25, and the new vessel in series 26 through 34.

transition region. The temperature increment of each measurement may be deduced from the adjacent mean temperatures and it is sufficiently small to ignore the curvature correction in comparison with the experimental precision. After each energy input was over, thermal equilibrium within calorimeter vessel was attained in 1 min below 10 K, in 5 min at 50 K, and 15 min above 100 K in the measurements using the old calorimeter vessel as well as the new vessel. There was nothing anomalous concerning thermal equilibration in the transition regions contrary to the observation of Dworkin and Cailleau,[31] and in the lowest temperature region either, where the possibility of the "incommensurate glass" was suggested by Liu and Conradi.[41] Although our results are systematically larger by 0.4 per cent than the data reported by Huffman et al.,[62] the two sets of data are in satisfactory agreement within combined experimental uncertainties where comparison can be made.

Some molar thermodynamic functions derived from the measured data are tabulated in Table 2, where small contribution below 4 K was estimated by smooth extrapolation from the higher temperature side. The calorimetric standard entropy of biphenyl in the standard ideal gas state was calculated using the vapor pressure[63] and sublimation[64] data as summarized in Table 3.

Twist Transition. Generally, a small anomaly in a heat capacity curve can be made more prominent by plotting the equivalent Debye characteristic temperatures corresponding to the heat capacity values. It is shown in Fig. 2, where it is arbitrarily assumed that there are 9 degrees of freedom per molecule. A small, broad minimum is seen at about 40 K in Fig. 2. The normal portion of the heat capacity was evaluated by drawing a smooth interpolating curve as the lower and the higher temperature sides guide the eyes as shown by the solid curve in Fig. 2. This graph was used to separate the excess heat capacities that are shown in Fig. 3. The anomaly is very broad extending from 30 K to 47 K with a maximum at (40.4±0.2) K. The enthalpy and the entropy of transition were determined as (5.02±0.08) J·mol^{-1} and (0.129±0.003) J·K^{-1}·mol^{-1}, respectively, by graphical integration of the excess heat capacities.

Biphenyl is known to show the twist transition of

Table 2. Molar Thermodynamic Functions of Biphenyl

T	$C_{p,m}$	$[H^\circ_m(T)-H^\circ_m(0)]/T$	$S^\circ_m(T)-S^\circ_m(0)$	$-[G^\circ_m(T)-H^\circ_m(0)]/T$
K	J K^{-1} mol^{-1}	J K^{-1} mol^{-1}	J K^{-1} mol^{-1}	J K^{-1} mol^{-1}
5	0.504	0.133	0.173	0.040
10	3.26	0.90	1.21	0.32
20	14.68	4.75	6.71	1.96
30	27.46	10.21	15.11	4.89
40	38.63	15.97	24.59	8.62
50	46.42	21.30	34.07	12.77
60	53.43	26.08	43.17	17.08
70	59.57	30.44	51.87	21.44
80	65.19	34.44	60.20	25.76
90	70.44	38.14	68.18	30.04
100	75.57	41.63	75.87	34.24
110	80.72	44.95	83.31	38.36
120	85.83	48.14	90.56	42.41
130	90.89	51.24	97.63	46.39
140	96.23	54.26	104.56	50.30
150	101.53	57.23	111.38	54.14
160	107.11	60.18	118.11	57.93
170	112.85	63.11	124.77	61.67
180	118.82	66.03	131.39	65.36
190	124.75	68.97	137.97	69.00
200	130.90	71.91	144.53	72.62
210	137.21	74.87	151.07	76.20
220	143.68	77.85	157.60	79.75
230	150.49	80.86	164.13	83.28
240	157.19	83.90	170.68	86.78
250	163.77	86.96	177.23	90.27
260	170.73	90.05	183.79	93.74
270	177.90	93.17	190.37	97.20
280	185.10	96.33	196.97	100.64
290	192.30	99.51	203.59	104.08
300	199.50	102.72	210.23	107.50
298.15	198.17	102.13	209.00	106.87

Table 3. Calorimetric Entropy of Biphenyl

	S°_m/J K^{-1} mol^{-1}
0 to 4 K (smooth extrapolation)	0.089
4 to 298.15 K (graphical)	208.9
Sublimation[a]	274.2
Entropy of real gas at 298.15 K	483.2
Compression[b] and correction to ideal gas[c]	−93.7
S°_m(biphenyl, 298.15 K, g, p=100000 Pa)	389.5

a) $\Delta_{vap}H$=81760 J · mol^{-1} at 298.15 K.[64] b) p=1.30 Pa at 298.15 K.[63] c) Using Berthelot's equation of state.

Table 4. Properties of the Successive Phase Transitions of Biphenyl

	Lock-in transition	Twist transition
T_{trs}/K	16.8±0.1	40.4±0.2
Region/K	15.3–18.3	30–47
$\Delta_{trs}H$/J mol^{-1}	0.15±0.02	5.02±0.08
$\Delta_{trs}S$/J K^{-1} mol^{-1}	0.009±0.001	0.129±0.003

the displacive type associated with some soft-modes.[24–27] The properties of the twist transition in biphenyl are summarized in Table 4. The shape of the anomaly and the smallness of the entropy of transition are consistent with the higher-order, displacive nature of the twist transition. On the other hand, *p*-terphenyl and *p*-quaterphenyl crystals undergo the twist transition of the order-disorder type[21,65] at much higher temperatures (193.5 K[66] and 233.0 K,[55] respectively) compared with biphenyl. The heat capacity anomalies of biphenyl and *p*-quaterphenyl are both very broad but that of *p*-terphenyl is

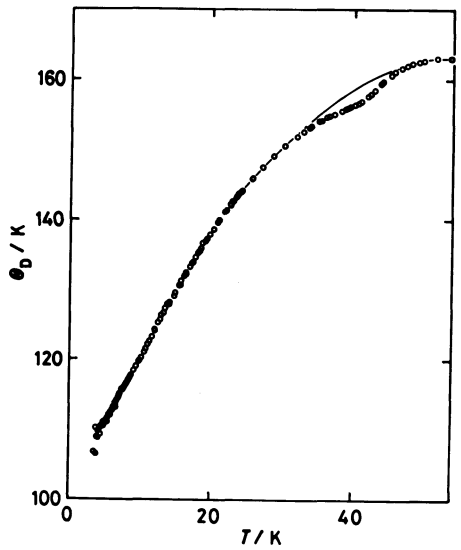

Fig. 2. Debye characteristic temperatures corresponding to the measured heat capacities of biphenyl assuming 9 degrees of freedom per molecule.

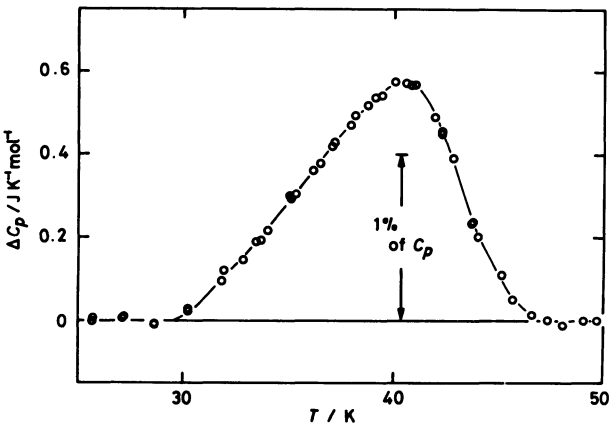

Fig. 3. Excess heat capacities due to the twist transition of biphenyl.

sharp.[66-68] The behavior of the three substances has been discussed[55] in terms of the molecular symmetry and the potentials for the intramolecular twisting modes.

Lock-in Transitions. No anomaly corresponding to the lock-in transition can be discerned in Fig. 2, which are the results obtained by using the old calorimeter vessel; the slight distortion at about 11 K is probably due to a failure in the germanium temperature scale.[51,52] The results of measurements using the new vessel are shown in Fig. 4 in the form of θ_D plot, where the data obtained in series 34 of measurements are shown. In this series, the temperature increment of each measurement was about 0.2 K. A broad anomaly is now clearly seen. The excess heat capacities were then separated by drawing the normal portion as shown by the solid

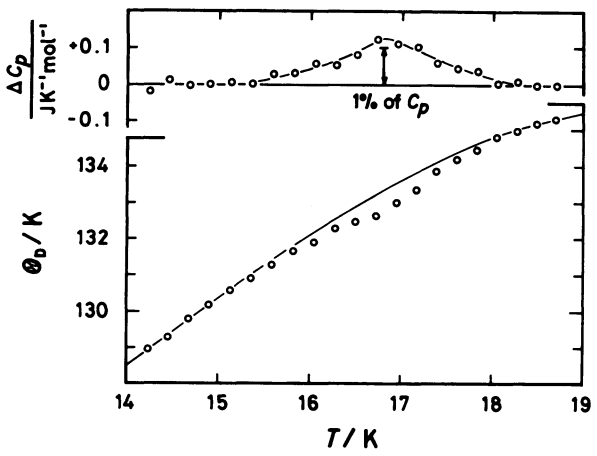

Fig. 4. Shape of the anomaly due to the lock-in transition of biphenyl (data of a typical run).

curve. The anomaly is broad extending from 15.3 K to 18.3 K with a maximum at (16.8±0.1) K, showing a large tail on the high temperature side. The enthalpy and the entropy of transition were determined as (0.15±0.02) J·mol^{-1} and (0.009±0.001) J·K^{-1}·mol^{-1}, respectively. This transition obviously corresponds to the reported lock-in transition by which the lattice becomes commensurate except for the b^* direction. The properties of the lock-in transition are also summarized in Table 4.

The shape of the anomaly and the smallness of the entropy of transition suggest that the lock-in transition is a higher-order transition. However, some evidences that the lock-in transition is of the first-order have been reported,[28,34,38] and the Landau's phenomenology[45,48] also predicts that it must be so. The present heat capacity results are smooth to within ±0.1 per cent at the top of the anomaly, 16.8 K, and there was no indication of latent heat. Similar discrepancy was reported in the case of K_2SeO_4.[69] There are two possible explanations of such a discrepancy on the notion that the transition is in fact of the first order. One is that the latent heat is so small that its effect is not reflected in the heat capacity runs. As one sees from the upper portion of Fig. 4, the anomalous part is smooth to within about 0.1 per cent; therefore the latent heat, if any, must be smaller than about 0.01 J·mol^{-1}. The other possibility, which is more likely, is that crystallites have a different lock-in transition temperature, i.e. the overall heat effects are smeared.

The large tail on the higher temperature side at the lock-in transition has been observed also in other substances,[69-71] and it may be accompanied with discommensuration mechanism proposed by McMillan.[72]

No further anomaly was found at lower temperatures in spite of a search for the other lock-in transition in the direction of the b^* axis. Any

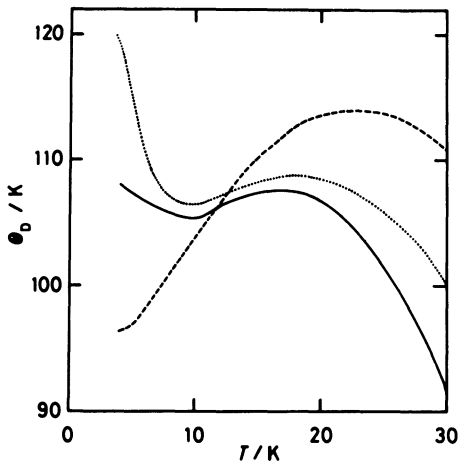

Fig. 5. Debye characteristic temperatures corresponding to the measured heat capacities of biphenyl (broken curve), *p*-terphenyl (solid curve) and 4,4′-difluorobiphenyl (dotted curve) assuming 6 degrees of freedom per molecule.

indication of freezing of some motional degrees of freedom was not observed either.[41] A simple interpretation of this fact is that the lock-in transition in the *b** direction could exist below 3 K, the lowest temperature reached in the present experiments. The other, more tempting interpretation is that the incommensurate phase could be stable down to the absolute zero. If the latter is the case, the crystal would represent a new type of thermodynamic stability. Determination of the spectroscopic entropy in the gas phase will give us a clue to this problem. It must be emphasized, however, the "residual entropy," if present, is expected to be very small taking the smallness of the entropy of lock-in transitions into account.

Crossover of Low Temperature Heat Capacities. The comparison of the low temperature heat capacities of biphenyl and *p*-terphenyl[53,66] is shown in Fig. 5 in terms of corresponding Debye characteristic temperatures assuming 6 degrees of freedom per molecule. Below about 20 K, the heat capacity of biphenyl decreases less steeply than that of *p*-terphenyl as the temperature decreases, and they cross each other at about 12 K. The crossover between biphenyl and *p*-quaterphenyl was also observed at about 6 K.[55]

Since biphenyl and *p*-terphenyl have similar crystal structures and their intermolecular interactions are also similar, one would expect that the relative magnitude of their heat capacities is determined primarily by the relative molecular mass, i.e. the heavier molecule should show a larger heat capacity at a low temperature, where only low-lying lattice modes are excited. Therefore, there must be some motional mode or modes in biphenyl for which the force constant is much smaller than for the corresponding mode(s) in *p*-terphenyl. The twisting mode about the central C–C bond in biphenyl seems to be the candidate of such a mode because (1) it is the only conceivable intramolecular mode that is susceptible to the crystal field, (2) the coupling of the twisting motion with the lattice vibration has been pointed out in many experimental[73–75] and theoretical[46,73,74,76,77] studies on the lattice vibrations of biphenyl crystal, and (3) the twisted conformation in *p*-terphenyl has been substantiated[20,23] below the order-disorder transition[21,65] in contrast with biphenyl. Thus, an attempt will be made to interpret the observed crossover by a simple model calculation of lattice vibration spectra for biphenyl and *p*-terphenyl crystals.

For biphenyl the average crystal structure at 22 K[15] was used, ignoring the incommensurability which will play an important role only in the very low temperature region where the contribution of phason becomes dominant.[78] The structure of *p*-terphenyl at 113 K[20] was corrected for thermal expansion down to 22 K by a linear extrapolation from the room temperature data.[21]

The intermolecular interaction was expressed by the sum of atom–atom pair potentials of Buckingham type, in which the parameters were taken from the literature.[79] The interactions were summed over molecules within a radius of 1 nm. Phenyl rings were assumed to be rigid.

The Lagrangian L of the system was written in terms of translational (superscript; t), rotational (r), and twisting (τ) coordinates in the harmonic approximation as follows:[80]

$$L = K - \Phi,$$

$$K = \frac{1}{2}\sum_{l}\sum_{\kappa}\sum_{\alpha} m\,[\,\dot{u}^{t}_{\alpha}(l\kappa)\,]^2 + \frac{1}{2}\sum_{l}\sum_{k}\sum_{\alpha,\beta} I_{\alpha\beta}(\kappa)\,\dot{u}^{r}_{\alpha}(l\kappa)\,\dot{u}^{r}_{\beta}(l\kappa) + \frac{1}{2}\sum_{l}\sum_{\kappa} I_{\tau}\,[\,\dot{u}^{\tau}(l\kappa)\,]^2,$$

$$\Phi = \Phi_0 + \frac{1}{2}\sum_{l,l'}\sum_{\kappa,\kappa'}\sum_{\alpha,\beta} \phi^{tt}_{\alpha\beta}(l\kappa; l'\kappa')\,u^{t}_{\alpha}(l\kappa)\,u^{t}_{\beta}(l'\kappa') + \frac{1}{2}\sum_{l,l'}\sum_{\kappa,\kappa'}\sum_{\alpha,\beta} \phi^{tr}_{\alpha\beta}(l\kappa; l'\kappa')\,u^{t}_{\alpha}(l\kappa)\,u^{r}_{\beta}(l'\kappa') + \frac{1}{2}\sum_{l,l'}\sum_{\kappa,\kappa'}\sum_{\alpha,\beta} \phi^{rt}_{\alpha\beta}(l\kappa; l'\kappa')\,u^{r}_{\alpha}(l\kappa)\,u^{t}_{\beta}(l'\kappa') + \frac{1}{2}\sum_{l,l'}\sum_{\kappa,\kappa'}\sum_{\alpha,\beta} \phi^{rr}_{\alpha\beta}(l\kappa; l'\kappa')\,u^{r}_{\alpha}(l\kappa)\,u^{r}_{\beta}(l'\kappa')$$

$$+\frac{1}{2}\sum_{l,l'}\sum_{\kappa,\kappa'}\sum_{\alpha} \phi_{\alpha}^{t\tau}(l\kappa;l'\kappa')u_{\alpha}^{t}(l\kappa)u^{\tau}(l'\kappa')$$

$$+\frac{1}{2}\sum_{l,l'}\sum_{\kappa,\kappa'}\sum_{\alpha} \phi_{\alpha}^{\tau t}(l\kappa;l'\kappa')u^{\tau}(l\kappa)u_{\alpha}^{t}(l'\kappa')$$

$$+\frac{1}{2}\sum_{l,l'}\sum_{\kappa,\kappa'}\sum_{\alpha} \phi_{\alpha}^{t\tau}(l\kappa;l'\kappa')u_{\alpha}^{r}(l\kappa)u^{\tau}(l'\kappa')$$

$$+\frac{1}{2}\sum_{l,l'}\sum_{\kappa,\kappa'}\sum_{\alpha} \phi_{\alpha}^{\tau r}(l\kappa;l'\kappa')u^{\tau}(l\kappa)u_{\alpha}^{r}(l'\kappa')$$

$$+\frac{1}{2}\sum_{l,l'}\sum_{\kappa,\kappa'} \phi^{\tau\tau}(l\kappa;l'\kappa')u^{\tau}(l\kappa)u^{\tau}(l'\kappa')$$

$$\phi_{\alpha\beta}^{ab}(l\kappa;l'\kappa') = \frac{\partial^2\Phi}{\partial u_{\alpha}^{a}(l\kappa)\,\partial u_{\beta}^{b}(l'\kappa')},$$

where u is the displacement from an equilibrium position and α and β mean x, y, or z permutatively. Thus, $u_{\alpha}(l\kappa)$ denotes the displacement of the κ-th molecule in the l-th cell in the direction α. The equations of motion derived from the Lagrangian were numerically solved for 512 points picked up uniformly in the first Brillouin zone.

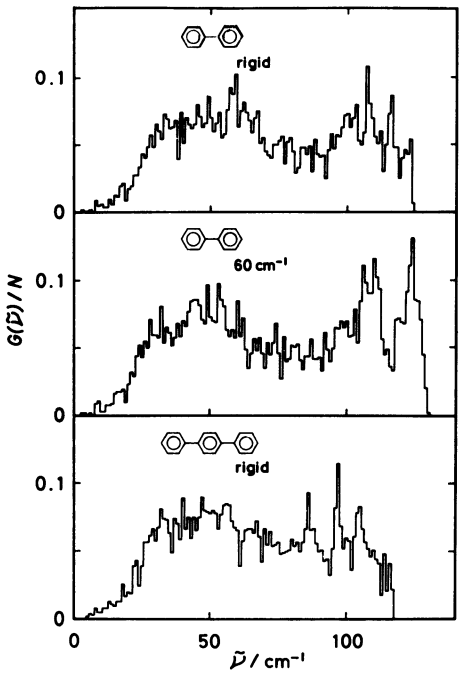

Fig. 6. Calculated density of states for rigid biphenyl, flexible biphenyl and rigid p-terphenyl.

The results of calculation are shown in Figs. 6 and 7. On the assumption of the rigid body, where there are no terms involving the twisting coordinates in the Lagrangian, p-terphenyl shows larger heat capacities than biphenyl at all the temperatures, as expected from the relative molecular mass. However, when one introduces flexibility into the biphenyl molecule with regard to the twisting of phenyl rings (a force constant corresponding to 60 cm^{-1} as the intramolecular contribution), biphenyl comes to show higher density of states in the low frequency region. On the other hand, p-terphenyl has higher density between 25 and 45 cm^{-1} due to its larger mass. Figure 7 shows the Debye temperature curve calculated from the spectra of Fig. 6 and the twisting flexibility is reflected in the crossover in the heat capacities at about 12 K. Now, we conclude qualitatively that the crossover can be attributed to the low-frequency twisting mode contribution of phenyl rings in biphenyl.

The same interpretation applies to the comparison between biphenyl and 4,4′-difluorobiphenyl which also has an analogous crystal structure at room temperature.[54,81–83]

The behavior of the Debye temperature of 4,4′-difluorobiphenyl[56] assuming 6 degrees of freedom per molecule is also shown in Fig. 5. The heat capacity of biphenyl is larger than that of 4,4′-difluorobiphenyl below about 13 K in spite of the smaller mass of the former molecule.[56] Thus, it is clear that the heat capacities of biphenyl crystal are much larger at low temperatures than those of the homologous molecules and derivatives. Therefore, the central C–C bond of biphenyl is extremely soft with regard to the internal rotation: The competing effect of the intra- and intermolecular interactions is very subtle and it plays

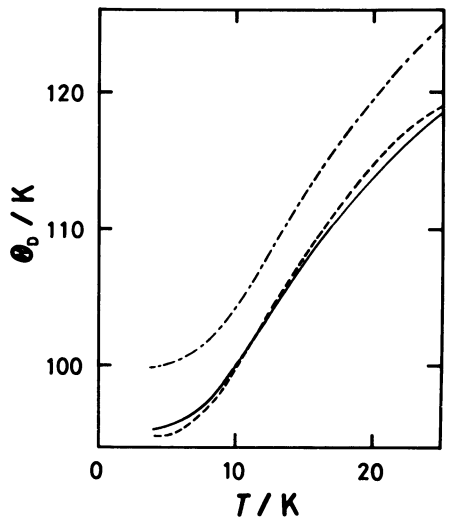

Fig. 7. Calculated Debye characteristic temperatures of rigid p-terphenyl(solid curve), flexible biphenyl (broken curve) and rigid biphenyl (dot-dash curve), assuming 6 degrees of freedom per molecule.

a critical role in the incommensurate structure of the crystal in such a way that the twisting mode in strongly coupled to the lattice vibration to such as extent that is not realized in similar other molecules.

References

1) O. Bastiansen, *Acta Chem. Scand.*, **3**, 408 (1949).
2) H. Suzuki, *Bull. Chem. Soc. Jpn.*, **32**, 1340 (1959).
3) J. Dale, *Acta Chem. Scand.*, **11**, 640 (1957); **11**, 650 (1957).
4) V. J. Eaton and D. Steele, *J. Chem. Soc., Faraday Trans. 2*, **69**, 1601 (1973).
5) A. J. Grumadas, D. P. Poshkus, and A. V. Kiselev, *J. Chem. Soc., Faraday Trans. 2*, **75**, 1398 (1979).
6) A. J. Grumadas, D. P. Poshkus, and A. V. Kiselev, *J. Chem. Soc., Faraday Trans. 2*, **78**, 2013 (1982).
7) G. L. Clark and L. W. Pickett, *J. Am. Chem. Soc.*, **53**, 167 (1931).
8) J. Dhar, *Indian J. Phys.*, **7**, 43 (1932).
9) J. Trotter, *Acta Crystallogr.*, **14**, 1135 (1961).
10) G. B. Robertson, *Nature (London)*, **191**, 593 (1961).
11) A. Hargreaves and S. H. Rizvi, *Acta Crystallogr.*, **15**, 365 (1962).
12) V. M. Kozhin and K. V. Mirskaya, *Sov. Phys. Crystallogr.*, **14**, 938 (1970).
13) G. P. Charboneau and Y. Delugeard, *Acta Crystallogr., Sect. B*, **32**, 1420 (1976).
14) G. P. Charboneau and Y. Delugeard, *Acta Crystallogr., Sect. B*, **33**, 1586 (1977).
15) H. Cailleau, J. L. Baudour, and C. M. E. Zeyen, *Acta Crystallogr., Sect. B*, **35**, 426 (1979).
16) J. L. Baudour and M. Sanquer, *Acta Crystallogr., Sect. B*, **39**, 75 (1983).
17) V. Petricek, P. Coppens, and P. Becker, *Acta Crystallogr., Sect. A*, **41**, 478 (1985).
18) H. M. Rietveld, E. N. Maslen, and C. J. B. Clews, *Acta Crystallogr., Sect. B*, **26**, 693 (1970).
19) J. L. Baudour, *Acta Crystallogr., Sect. B*, **28**, 1649 (1972).
20) J. L. Baudour, Y. Delugeard, and H. Cailleau, *Acta Crystallogr., Sect. B*, **32**, 150 (1976).
21) J. L. Baudour, H. Cailleau, and W. B. Yelon, *Acta Crystallogr., Sect. B*, **33**, 1773 (1977).
22) Y. Delugeard, J. Desuche, and J. L. Baudour, *Acta Crystallogr., Sect. B*, **32**, 702 (1976).
23) J. L. Baudour, Y. Delugeard, and P. Rivet, *Acta Crystallogr., Sect. B*, **34**, 625 (1978).
24) P. S. Friedman, P. Kopelman, and P. N. Prasad, *Chem. Phys. Lett.*, **24**, 15 (1974).
25) A. Bree and M. Edelson, *Chem. Phys. Lett.*, **46**, 500 (1977).
26) M. Wada, A. Sawada, and Y. Ishibashi, *J. Phys. Soc. Jpn.*; **50**, 737 (1980).
27) H. Cailleau, A. Girard, F. Moussa, and C. M. E. Zeyen, *Solid State Commun.*, **29**, 259 (1979).
28) H. Cailleau, F. Moussa, and J. Mons, *Solid State Commun.*, **31**, 521 (1979).
29) H. Cailleau, J. C. Messager, F. Moussa, F. Bugaut, C. M. E. Zeyen, and C. Vettier, *Ferroelectrics*, **67**, 3 (1986).
30) A. Janner, T. Janssen, and P. M. de Wolff, *Acta Crystallogr., Sect. A*, **39**, 671 (1983).
31) A. Dworkin and H. Cailleau, *J. Phys. (Paris) Lett.*, **41**, L-83 (1980).
32) A. S. Cullick and R. E. Gerkin, *Chem. Phys.*, **23**, 217 (1977).
33) A. S. Cullick and R. E. Gerkin, *Chem. Phys. Lett.*, **42**, 589 (1976).
34) A. Bree and M. Edelson, *Chem. Phys. Lett.*, **55**, 319 (1978).
35) N. I. Wakayama, *Chem. Phys. Lett.*, **83**, 413 (1981).
36) C. Ecolivet, M. Sanquer, J. Pellegrin, and J. DeWitte, *J. Chem. Phys.*, **78**, 6317 (1983).
37) D. Kirin, S. L. Chaplot, G. A. Mackenzie, and G. S. Pawley, *Chem. Phys. Lett.*, **102**, 105 (1983).
38) J. L. Baudour, L. Toupet, Y. Delugeard, and S. Ghemid, *Acta Crystallogr., Sect. C*, **42**, 1211 (1986).
39) V. Heine and S. L. Price, *J. Phys. C*, **18**, 5259 (1985).
40) H. Cailleau, F. Moussa, C. M. E. Zeyen, and J. Bouillot, *Solid State Commun.*, **33**, 407 (1980).
41) S. B. Liu and M. S. Conradi, *Phys. Rev. Lett.*, **54**, 1287 (1985).
42) C. Benkert and V. Heine, *Phys. Rev. Lett.*, **58**, 2232 (1987).
43) H. Cailleau, A. Girard, J. C. Messager, Y. Delugeard, and C. Vettier, *Ferroelectrics*, **54**, 257 (1984).
44) R. M. Hochstrasser, R. D. McAlpine, and J. D. Whiteman, *J. Chem. Phys.*, **58**, 5078 (1973).
45) Y. Ishibashi, *J. Phys. Soc. Jpn.*, **50**, 1255 (1981).
46) N. M. Plakida, A. V. Belushkin, I. Natkaniec, and T. Wasiutyński, *Phys. Status Solidi B*, **118**, 129 (1983).
47) W. R. Busing, *Acta Crystallogr., Sect. A*, **39**, 340 (1983).
48) P. Toledano and M. Guilluy, *Ferroelectrics*, **53**, 311 (1984).
49) J. C. Raich and E. R. Bernstein, *Mol. Phys.*, **53**, 597 (1984).
50) T. Janssen, *Jpn. J. Appl. Phys.*, **24**, Suppl. 24-2, 747 (1985).
51) T. Atake and H. Chihara, *Solid State Commun.*, **35**, 131 (1980).
52) T. Atake, K. Saito, and H. Chihara, *Chem. Lett.*, **1983**, 493.
53) K. Saito, T. Atake, and H. Chihara, *Chem. Lett.*, **1984**, 521.
54) K. Saito, H. Chihara, T. Atake, and Y. Saito, *Jpn. J. Appl. Phys.*, **24**, Suppl. 24-2, 838 (1985).
55) K. Saito, T. Atake, and H. Chihara, *J. Chem. Thermodyn.*, **17**, 539 (1985).
56) K. Saito, T. Atake, and H. Chihara, *J. Chem. Thermodyn.*, **18**, 407 (1986).
57) K. Saito, T. Atake, and H. Chihara, *Thermochim. Acta*, **109**, 45 (1986).
58) K. Saito, T. Atake, and H. Chihara, *J. Chem. Thermodyn.*, **19**, 9 (1987).
59) K. Saito, T. Atake, and H. Chihara, *J. Chem. Thermodyn.*, **19**, 633 (1987).
60) T. Atake and H. Chihara, *Bull. Chem. Soc. Jpn.*, **47**, 2126 (1974).
61) T. Atake and H. Chihara, (unpublished).
62) H. G. Huffman, G. S. Parks, A. C. Daniels, *J. Am. Chem. Soc.*, **52**, 1547 (1930).
63) R. S. Bradley and T. G. Cleasby, *J. Chem. Soc.*, **1953**, 1690.
64) E. Morawetz, *J. Chem. Thermodyn.*, **4**, 455 (1972).

65) B. A. Bolton and P. N. Prasad, *Chem. Phys.*, **35**, 331 (1978).
66) K. Saito, T. Atake, and H. Chihara, (unpublished).
67) H. Cailleau and A. Dworkin, *Mol. Cryst. Liq. Cryst.*, **50**, 217 (1979).
68) S. S. Chang, *J. Chem. Phys.*, **79**, 6229 (1983).
69) K. Nomoto, T. Atake, B. K. Chaudhuri, and H. Chihara, *J. Phys. Soc. Jpn.*, **52**, 3475 (1983).
70) T. Atake, K. Nomoto, B. K. Chaudhuri, and H. Chihara, *J. Chem. Thermodyn.*, **15**, 339 (1983).
71) T. Atake, K. Nomoto, B. K. Chaudhuri, and H. Chihara, *J. Chem. Thermodyn.*, **15**, 383 (1983).
72) W. L. McMillan, *Phys. Rev. B*, **14**, 1496 (1976).
73) I. Natkaniec, A. V. Belushkin, and T. Wasiutyński, *Phys. Status Solidi B*, **105**, 413 (1981).
74) H. Takeuchi, S. Suzuki, A. J. Dianoux, and G. Allen, *Chem. Phys.*, **55**, 153 (1981).
75) A. V. Belushkin, I. Natkaniec, J. Wasicki, and T. Zaleski, *Phys. Status Solidi B*, **123**, K115 (1984).
76) E. Burgos, H. Bonadeo, and E. D'Alessio, *J. Chem. Phys.*, **65**, 2460 (1976).
77) H. Bonadeo and E. Burgos, *Acta Crystallogr., Sect. A*, **38**, 29 (1982).
78) M. L. Boriack and A. W. Overhauser, *Phys. Rev. B*, **18**, 6454 (1978).
79) D. E. Williams, *J. Chem. Phys.*, **47**, 4680 (1967).
80) G. Venkataraman and V. C. Sahni, *Rev. Mod. Phys.*, **42**, 409 (1970).
81) T. K. Halstead, H. W. Spiess, and U. Haeberlen, *Mol. Phys.*, **31**, 1569 (1976).
82) T. K. Halstead, J. Tagenfeldt, and U. Haeberlen, *J. Chem. Soc., Faraday Trans. 2*, **77**, 1817 (1981).
83) K. Saito, T. Atake, and H. Chihara, *Acta Crystallogr., Sect. B*, **43**, 383 (1987).